KSCE Journal of Civil Engineering (2013) 17(4):651-661
DOI 10.1007/s12205-013-1591-3

Geotechnical Engineering
www.springer.com/12205

Self-balanced Earthquake Simulator on Centrifuge and Dynamic Performance Verification

Dong-Soo Kim*, Sei-Hyun Lee, Yun Wook Choo***, and Jacques Perdriat******

Received May 25, 2011/Revised May 1, 2012/Accepted May 29, 2012

Abstract

This paper describes some details of a self-balanced earthquake simulator on the centrifuge in KAIST and results of a series of proof tests for verifying its dynamic performance and excitation capacity. The main feature of the earthquake simulator is the dynamic self-balancing technique adopted to eliminate a large portion of the undesired reaction forces and vibrations transmitted to the centrifuge main body. This feature is achieved by embarking counter-weight platform and two back-to-back hydraulic bearings. The maximum base shaking acceleration of the earthquake simulator is 20 g in horizontal direction under 40 g of centrifuge acceleration with a maximum payload of 700 kg, corresponding to 0.5 g of horizontal shaking acceleration in the prototype scale. The loading frequency ranges from 40 Hz to 200 Hz (300 Hz) for sinusoidal (real earthquake) inputs. The dimension of slip table is 670 mm × 670 m in length and width. The proof test results show that the earthquake simulator can reproduce mono-frequency sinusoidal inputs in a wide band of frequencies as well as multi-frequency real earthquake inputs at the bottom of soil models with satisfactory fidelity, and the dynamic self-balancing contributes to the safety of the centrifuge structure.

Keywords: *earthquake simulator, geotechnical centrifuge, self-balancing technique, earthquake, dynamic performance*

1. Introduction

It is well-known that an earthquake is capable of causing seismic hazards such as property damage and even the loss of lives, much of which is related to the failure of soil-structure systems or geotechnical structures. Significant efforts have been made by geotechnical researchers in finding how to evaluate the seismic performance of geotechnical structures or soil-structure systems subjected to earthquake loadings. Although the most popular method for this purpose is computer-based numerical modeling, reduced-scale physical modeling using a single gravity (1-G) shaking table or a dynamic geotechnical centrifuge facility is often employed to simulate earthquake-related geotechnical problems (Wood *et al*., 2002; Elgamal *et al*., 2005; Kutter and Wilson, 2006; Ghosh and Madabhushi, 2007; Yu *et al*., 2008; Ueng *et al*., 2010).

In the 1-G shaking table tests, the model is mounted on a massive bottom-fixed platform and is shaken by a set of servo-hydraulic actuators so as to apply appropriate input base motions. There are large numbers of possibilities for shaking table conceptions, mainly defined by the number of degrees of freedom under control. Consequently, there are shaking tables having from a single degree of freedom (typically, a horizontal translation) up to the more complex where the six degrees of freedom are simultaneously controlled (three translations and three rotations). These generate relatively accurate inertia forces and dynamic responses throughout. However, the inability to replicate the behavior of the full-scale prototype due to the difference of the self-weight stress level still remains the major drawback for 1-G shaking table tests.

In the geotechnical centrifuge tests, when a small scale soil model is accelerated to the appropriate multi g-level, the self-weight of the soil can be raised to the prototype scale stress field and the entire behavior of the model can be similar to that of full scale geotechnical structure. It is now generally accepted that an earthquake simulator mounted on a geotechnical centrifuge, namely, a dynamic geotechnical centrifuge is a valuable technique for obtaining reliable data under well-controlled testing conditions. And, it helps geotechnical engineers and researchers understand the mechanisms by which earthquake shaking affects the performance of soil-structure systems. A dynamic geotechnical centrifuge is also relevant for conducting parametric studies and

*Member, Professor, Dept. of Civil and Environmental Engineering, Korea Advanced Institute of Science and Technology (KAIST), Daejeon 305-701, Korea (E-mail: dskim@kaist.ac.kr)
**Senior Researcher, Dept. of Structural System & Site Evaluation, Korea Institute of Nuclear Safety (KINS), Daejeon 305-338, Korea (Corresponding Author, E-mail: lsh908@kins.re.kr)
***Research Professor, Dept. of Civil and Environmental Engineering, Korea Advanced Institute of Science and Technology (KAIST), Daejeon 305-701, Korea (E-mail: ywchoo@kaist.ac.kr)
****Member of the Board, Actidyn Systemes 1, Rue Du Groupe Manoukian, 78990 Elancourt, France (E-mail: jacques.perdriat@actidyn.com)

especially useful for validating numerical simulation tools, including constitutive models as well as boundary value problems.

However, it is difficult to accurately control the dynamic motions in the dynamic geotechnical centrifuge. The reason is that the centrifuge swinging basket is hinged to the centrifuge arm. Consequently, the reaction forces to the actuator excitations should be compensated within the basket. In addition, the shaking acceleration and frequency content of ground input motion have to be N times the prototype ground motion according to the scaling law (Taylor, 1995). Consequently, the maximum operating shaking acceleration and frequency usually range up to over 20 gh (gh denotes shaking acceleration unit in horizontal direction) and over 300 Hz, respectively. For such reasons, most of the in-flight earthquake simulators mounted on centrifuges are unidirectional while earthquake motions are multi-directional in nature. Currently, HKUST (Hong Kong University of Science and Technology) in Hong Kong and RPI (Rensselaer Polytechnic Institute) in the USA have a horizontally biaxial earthquake simulator (Shen *et al*., 1998; Zehgal *et al*., 2002), and UC Davis in the USA and TIT (Tokyo Institute of Technology) in Japan have a horizontal-vertically biaxial earthquake simulator (Kutter *et al*., 1994; Takemura *et al*., 2002).

Recently, a state-of-the-art geotechnical centrifuge facility has been installed at the Korea Advanced Institute of Science and Technology (KAIST) through the Korea Construction Engineering Development Collaboratory Program (KOCED program) funded by the Ministry of Land, Transport and Maritime Affairs of South Korea (Kim *et al*., 2013). The centrifuge facility was equipped with an electro-hydraulic servo type earthquake simulator capable of shaking in the horizontally biaxial directions. The earthquake simulator at KAIST has been actively operated to simulate seismic problems of a variety of geotechnical structures and soil-structure systems since January of 2010. For reliable applications, it is essential that the geotechnical engineer has a clear understanding of the apparatus and its performance capabilities and understands how the apparatus interacts with the test models. In this paper, composition details of the earthquake simulator as well as the main design concept of dynamic self-balancing are described. The dynamic performances, including the decoupling between the simulator and the centrifuge main body, are evaluated by the quality of replicating mono-frequency sinusoidal and multi-frequency recorded earthquake inputs. For the first stage, the performance verification is concentrated on horizontally unidirectional (1-D) shaking.

2. Self-balanced Earthquake Simulator at KAIST

2.1 Specification

A self-balanced electro-hydraulic earthquake simulator was mounted on the centrifuge, which has an effective radius of 5 m and a maximum capacity of 240 g-tons. The earthquake simulator was developed by a French manufacturer, Actidyn Systems, and is currently a unique apparatus capable of modeling seismic problems on the centrifuge in South Korea. It is designed to operate at up to 100 gc centrifugal acceleration, and the base shaking acceleration can be exerted to a maximum value of 20 gh at 40 gc (gc denotes unit for centrifugal acceleration) of centrifugal acceleration with a maximum payload of 700 kg, which corresponds to 0.5 gh in the prototype scale. The main specifications and general view of this earthquake simulator are shown in Table 1 and Fig. 1, respectively. The entire system was built in a separate centrifuge basket to equip the actuators and oil reservoirs for the dynamic model tests, and static basket should be replaced by the dynamic basket for the earthquake simulation on the centrifuge.

Table 1. Main Specifications of the Earthquake Simulator at KAIST

Items	Actidyn System Q72-2 Earthquake Simulator
Shaking Type	Electro hydraulic servo type
Shaking Direction	Two horizontal (X and Y)
Payload Dimension	0.67 m (Length) × 0.67 m (Width) × 0.65 m (Height)
Max. Model Payload	700 kg
Centrifuge Acceleration Range	10-100 gc
Max. Shaking Acceleration (No Payload)	40 gh
Max. Shaking Acceleration (Full Payload)	20 gh
Max. Displacement	6.5 mm
Max. Velocity	1.0 m/s
Loading Frequency Range (Random Vibration)	40-300 Hz
Loading Frequency Range (Sine Burst)	40-200 Hz

Fig. 1. Earthquake Simulator Mounted on the Centrifuge at KAIST

2.2 Dynamic Self-balancing Principle

Most classical earthquake simulators used the weight of the centrifuge swinging basket as a reaction mass. This would limit drastically the payload mass of the model in proportion to the weight of the basket in order to reduce the amplitude of undesired vibrations transmitted to the centrifuge basket and arms. Moreover, the centrifuge has its own mechanical resonance modes that must be avoided during seismic tests. When the excitation frequency of an experimental model coincides with

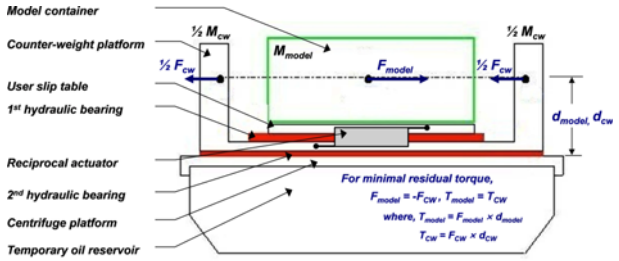

Fig. 2. Schematic Diagram of Dynamic Self-balancing Principle (after Pedriat *et al.*, 2002)

one of the resonance modes, the vibration resulting from the input excitation may causes permanent damage to the centrifuge structure or its components. Decoupling between the earthquake simulator and centrifuge arm is certainly required for the safety of the centrifuge structure.

The mechanical arrangement of the earthquake simulator at KAIST eliminates a large portion of the undesired reaction forces and vibrations by adopting the dynamic self-balancing principle (Pedriat *et al.*, 2002; Chazelas *et al.*, 2008). The earthquake simulator is composed of a user slip table carrying model payload and a Counter-Weight (CW) platform moving consistently in opposite phases. By embarking the counter-weight platform, the actuators are no longer established between the user slip table and the centrifuge platform, but between the user slip table and the counter-weight platform. As shown in Fig. 2, the counter-weight platform is decoupled from the user slip table and the centrifuge platform by two back-to-back hydraulic bearings. Dynamic self-balancing is achieved by a reciprocal actuation of the model payload and the counter-weights. Both moving masses have similar masses, with the center of mass at the same level from the platform (d_{model} and d_{cw}) and move horizontally in opposite directions at the same time in order to compensate the total torques. When the counteracting torques, T_{model} ($F_{model} \times d_{model}$) and T_{CW} ($F_{CW} \times d_{CW}$) are equal, the residual torque applied to the centrifuge platform is minimal. The dynamic self-balancing is important not only for simulating accurate input motion but for reducing the risk of damaging the mechanical parts of the centrifuge itself.

2.3 Mechanical and Hydraulic Components

Fig. 3 shows the mechanical assembly of the swinging basket with the earthquake simulator. There are four reciprocal hydraulic actuators in a symmetrical arrangement with two actuator pairs that are orthogonal to one another. Each actuator piston is equipped with a linear and a spherical hydrostatic slip bearing that provides friction free linear displacement along the X and Y axes and rotational displacement around the Z axis. In order to monitor the position of the piston, LVDT is internally installed in each actuator.

As shown in Fig. 2, the counter-weight platform which is supported by two back-to-back hydraulic bearings slides in a sandwich between the user slip table and the centrifuge base

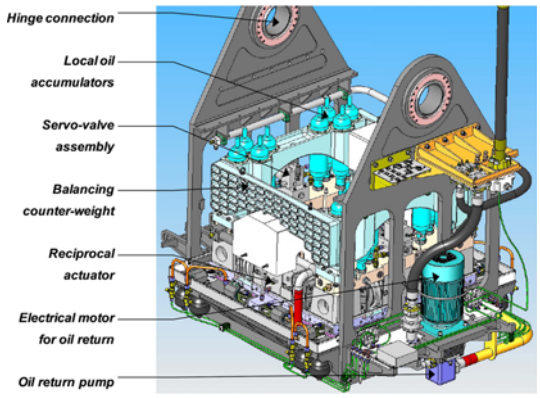

Fig. 3. Mechanical Assembly of the Swinging Basket

platform. This decoupling with the centrifuge base platform leads to the elimination of large rocking moment normally observed in classical non-reciprocating systems. The balancing counterweights shown in Fig. 3 are used to set up the center of mass of the model payload and counter-weight platform in the same horizontal plane. They are removable for easily mounting the model container on the slip table and are also adjustable to permit the center of mass alignment.

The hydraulic supply system consists of a hydraulic return pump, a set of local accumulators, manifolds, two high pressure hydraulic pumps, an oil reservoir, and an automatic control system. When dynamic tests are performed, it is necessary to supply a large amount of oil to the excitation system. To do that, the oil is supplied continuously from the oil reservoir in the hydro-electric power station to the local accumulators on the swinging basket through the rotary joints. The pressurized oil in the accumulators is exhaled in every instance of shaking. The oil used by the movement of the actuator pistons is stored in a temporary oil reservoir in the bottom of the basket and the hydraulic return pump periodically returns the oil to the external oil reservoir.

2.4 Computerized Control System

As shown in Fig. 4, the computerized control system consists

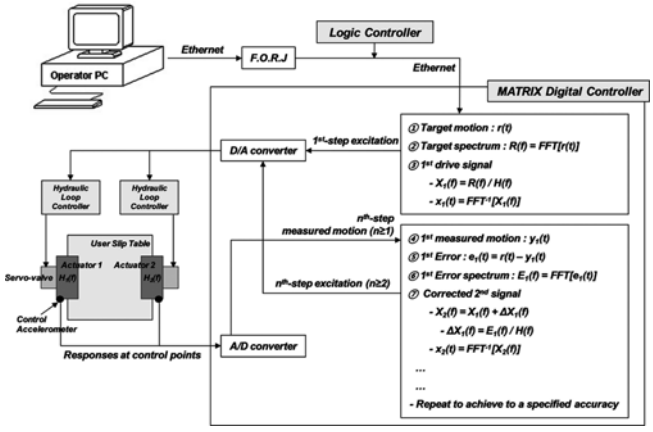

Fig. 4. Schematic Diagram of Computerized Control System

of three major parts: a logic controller, a set of hydraulic loop controllers, and a MATRIX digital controller. All the control systems are operated through a Fiber Optic Rotary Joint (FORJ) with a personal computer in the control room. The logic controller performs all logic functions required for the proper operation of the hydraulic power supply, the oil pressure, and flow control. It also governs all safety interlocks and fault detection, and interfaces directly with the centrifuge controller.

The hydraulic loop controllers that provide the control of servo-valves assembly operate cascade closed loops that typically incorporate the servo-valve spool position feedback, the actuator differential pressure, and the actuator acceleration feedback. The acceleration feedback signals are derived from ICP type accelerometers that are attached on one side of the actuators. The position feedback signal of the actuator is measured by the internal LVDT.

In general, the excitation on the earthquake simulator is not always in coincidence with a user-desired motion due to the complex mechanical assembly and mechanism. The SignalStar MATRIX digital controller, which is a dedicated digital control system from Data Physic Corporation, functions to generate an input signal and to correct the input signal so as to adjust excited responses to target responses based on the feedback information from the accelerometers and LVDT sensors (Hutin *et al*., 2002). The earthquake simulator has system dynamic characteristics that depend upon the inherent structural and hydraulic resonances of the system itself, as well as upon the type of input signal, the payload, and the operating conditions. First of all, a series of low level white noise signals that cause little change to model are sent to the hydraulic actuators to evaluate system dynamic characteristics (gain and phase information) using the measured signals at each accelerometer attached to the individual actuators X1, X2 & Y1, Y2.

The corresponding digital controller software generates actuator drive signals from a complex combination of user-desired signals and the measured system dynamic characteristics. To put it simply, the Fourier transformed target motions in acceleration, $Y(f)$, are divided by the system dynamics (acceleration/voltage frequency response function), $H(f)$, to obtain the Fourier transform of the input drive signal in voltage, $X(f)$. This can be inversely transformed to obtain the actual voltage drive signal, $x(t)$ needed to produce the target motion (reference motion, $r(t)$). Fig. 4 shows that an iterative scheme is required to estimate the correct input drive signal. It depends on the type, amplitude, and frequency content of the input motion, but usually two iterations are sufficient to achieve a good simulation of target motions, as will be described later in Section 3.2.

3. Proof Tests on Dyanamic Performance and Capacity

3.1 Test Model and Procedures

In order to examine the dynamic performance of the self-balancing earthquake simulator and its capacity, a series of proof tests were conducted with a soil model inside a model container as a payload. Dry sand was poured into the model container from a sand raining system to provide a fairly uniform sand layer. The total weight of the sand model including the model container was around 370 kg, and it corresponds to a relative density of around 80%. Fig. 5 shows cross-section views of the earthquake simulator and the sand model, as well as the instrumentation layout. Several accelerometers were used to determine the dynamic responses of the testing system. On the earthquake simulator, two accelerometers were attached on the head of the reciprocal actuators in X-direction (AX1, AX2) and a set of accelerometers which measure the on-axis shaking (Table-X), yawing (Table-Y), and rocking (Table-Z) accelerations, were placed at one end of the user slip table. In addition, one accelerometer on the counter-weight platform (CW-X) and two accelerometers on the end of the centrifuge arm (Arm-X, Arm-Z) were attached to examine the dynamic self-balancing technique and the safety of centrifuge structure. On the model payload, several accelerometers were embedded into the soil model at pre-determined locations during model preparation, as shown in Fig. 5(b). Five accelerometers, namely, from A1 to A5 were placed in two arrays, one at the middle of the soil deposit (Center) and the other on the inside of the end wall of the model container (Wall). In this study, the ESB (equivalent shear beam) model container first designed by Schofield and Zeng (1992) at University of Cambridge, was used in the proof tests. It was built with a stack of light-weight

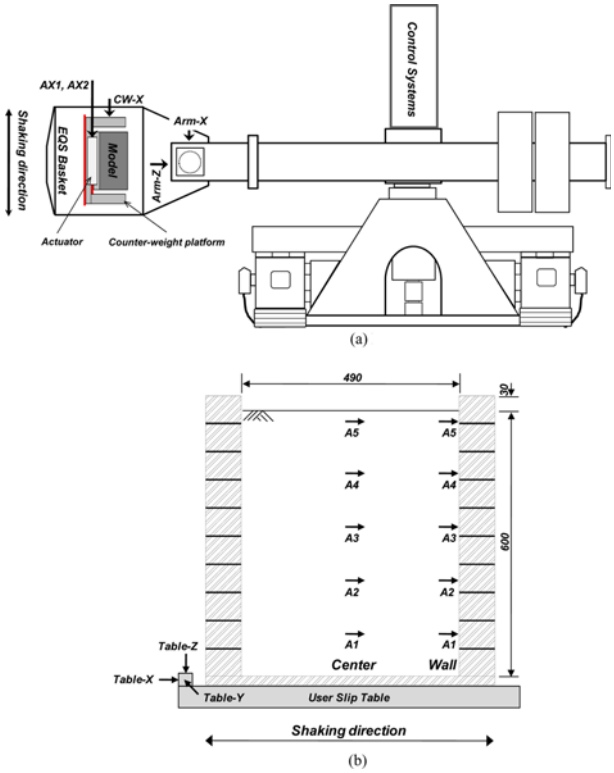

Fig. 5. KAIST Earthquake Simulator Including the Soil Model, and the Instrumentation Layout for Proof Tests: (a) KAIST Earth-Quake Simulator, (b) User Slip Table and Soil Model

Table 2. Summary of Performed Test Cases and Their Purposes

Test Cases	Excitation Type	Predominant Frequency (Hz)	Peak Amplitude (gh)	Purpose
Pretest	White Noise	-	0.3 Vrms[1)]	To determine the system dynamics
Northridge	Northridge EQ	165[2)]	2 ~ 20	To inspect the ability of the earthquake simulator for performing multi-frequency inputs To investigate boundary effects of ESB model container
Sin40	Sine Burst	40	2 ~ 16	To examine capacity and dynamic performance of the earthquake simulator for sine burst input signals
Sin80		80	2 ~ 20	
Sin100		100	2 ~ 20	
Sin120		120	2 ~ 10	
Sin140		140	2 ~ 10	
Sin160		160	2 ~ 20	
Sin180		180	2 ~ 10	

[1)]Maximum driving voltage of random white noise signal
[2)]Predominant frequency at centrifugal acceleration of 60 gc : about 2.7 Hz in prototype scale

aluminum frames separated by rubber layers in order to create flexible frictional end walls that have dynamic stiffness equivalent to that of the inside soil model. Consequently, it is expected that the end walls will provide the same dynamic responses with the soil model in the model container by minimizing the boundary effects. The accelerations at the Wall array can be compared with those at the Center array in order to evaluate the dynamic performance of the ESB model container. The internal dimension of the ESB model container is 490 mm × 490 mm × 630 mm in length, width, and height, respectively.

In this study, the dynamic geotechnical centrifuge tests were intensively performed at a centrifugal acceleration of 60 gc. Table 2 gives a summary of the performed test cases and their purposes. At first, in the pretest, a series of low level white noise signals were sent to the hydraulic actuators during spinning at 60 gc, and then the system dynamic characteristics (that is, transfer functions) were computed using the signals measured at the accelerometers on the shaking actuators. After the transfer functions were determined, the Northridge Earthquake, which occurred on January 17, 1994 in California, was applied in order to inspect the ability to perform multi-frequency inputs. The earthquake input data was calibrated beforehand according to scaling rules (Taylor, 1995). Assuming a centrifugal acceleration of N gravitation, the acceleration and the frequency content were scaled to N times the prototype, and the duration was scaled to $1/N$ times. The frequency contents were filtered between 40 Hz and 300 Hz based on the limited frequency bandwidth of the earthquake simulator indicated in Table 1. At 60 gc, the frequency bandwidth corresponds to that between around 0.7 Hz and 5 Hz in the prototype scale. The calibrated motion was loaded in stages from small to large amplitude according to the ranges of shaking acceleration given in Table 2. After that, a series of sinusoidal input signals that need more consumption of oil were applied with various amplitudes and frequencies in order to examine the capacity and the performance of the earthquake simulator. The single amplitudes of the sinusoidal signal were progressively increasing from 2 gh to around 20 gh and all excitations were continued for 1 second independent on the levels of amplitude and frequency.

3.2 Pretest Results and Signal Correction Process

In order to produce a target motion, the relationship between the input drive signal (voltage) and the corresponding output motion (g) must be known. In general, since this kind of testing system behaves in a nearly linear mode over a broad range of operating conditions, the problem of determining the input drive signal can be approximated by dividing the system output motion by the transfer function. In the pretest, the transfer function ($H(f)$), that is, the acceleration/voltage frequency response function can be computed as shown in Fig. 6. For this measurement, the soil model was excited by the random white noise signals of 0.3 V_{rms}, and 16 excitation records were averaged to improve the signal-to-noise ratio of the measurements. As shown in Fig. 6, the two hydraulic actuators performing the shaking in the X-direction have significantly different transfer functions. The magnitude of actuator 1 is larger than that of actuator 2 throughout all of the frequency ranges. This means that a larger voltage of drive signal should be sent to actuator 2 when a certain level of shaking motion is required to excite to the payload. The frequency range of around 180 Hz corresponds to the fundamental hydraulic resonance caused by the interaction of

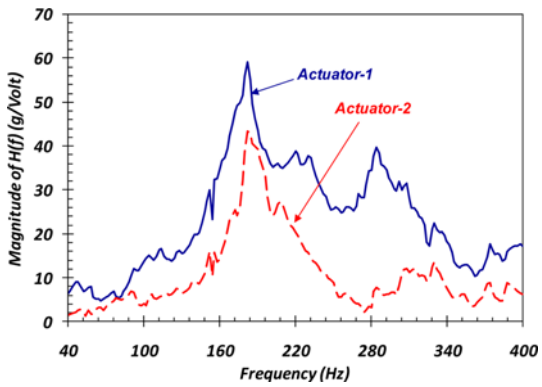

Fig. 6. Acceleration/Voltage Frequency Response Functions Determined in Pretest

the shaken mass including the model payload and the compliant hydraulic oil flow within the system. The peak magnitudes at around 180 Hz for both actuators and around 285 Hz for actuator 1 indicate that the earthquake simulator responds strongly and is, therefore, capable of producing large accelerations around these frequency ranges.

The initial drive signal at each level of acceleration is corrected by the iteration process shown in Fig. 4 in order to eliminate errors in terms of amplitude in the time domain and harmonics in the frequency domain. Generally, this process requires two models for each test: one dummy model to determine the right drive signals for the expected acceleration levels at the bottom of the container, and the other model for the real experiment. The drive signals computed from the dummy model are then replayed during real experiments. However, since this study focuses on examining the capacity of the earthquake simulator, all tests indicated in Table 2 were successively performed using one test model.

Figure 7 shows the corrections of the two actuator motions measured by sine burst excitation with 100 Hz frequency and 2 gh amplitude. The target motion was plotted together with actuator output motions in the time domain for comparative purposes. In the first trial, the actuator output motions were significantly distorted as compared with the target acceleration time history due to a lack of correction. On this account, the high amplitude harmonics were additionally observed at frequencies of 200 Hz and 300 Hz. However, as the correction process is iterated, the distortion in the time domain and the harmonics at high frequencies are gradually reduced to negligible levels, and the output motions match well with the target input motion. Moreover, the *RMS* (root mean square) values of the output are progressively close to the value of the target motion. Since this amplitude of 2 gh is not only very small acceleration in model scale but also the initial step of shaking acceleration in this study, four iterations were generally required to achieve good simulation of the target motion. However, usually, two iterations were enough to achieve a reasonably satisfactory result for the following steps of higher accelerations.

Figure 8 shows the correction process for the Northridge Earthquake excitation with 20 gh amplitude. Since this amplitude of 20 gh is the last acceleration step that experiences several corrections in the previous lower acceleration steps, even the first trial is satisfied with little difference from the target motion, and the second trial nearly matches the target motion throughout the

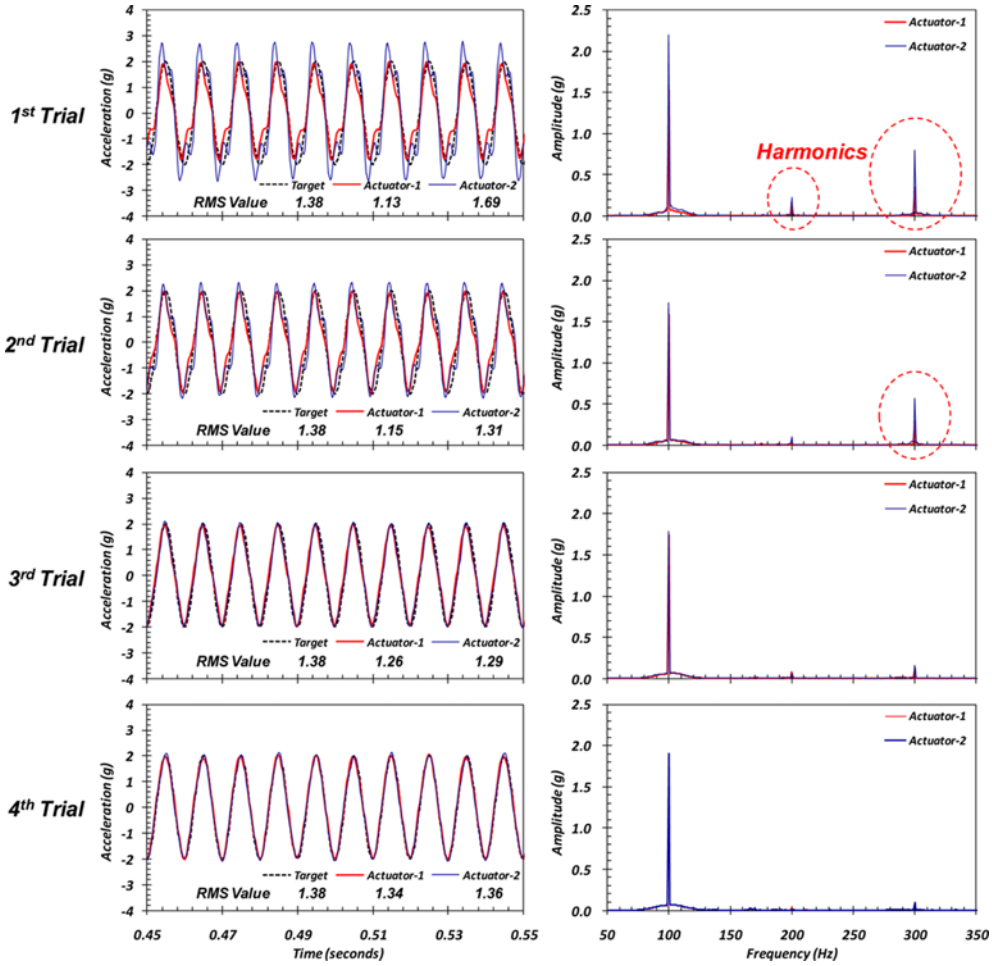

Fig. 7. Correction Process for Sine Burst Excitation

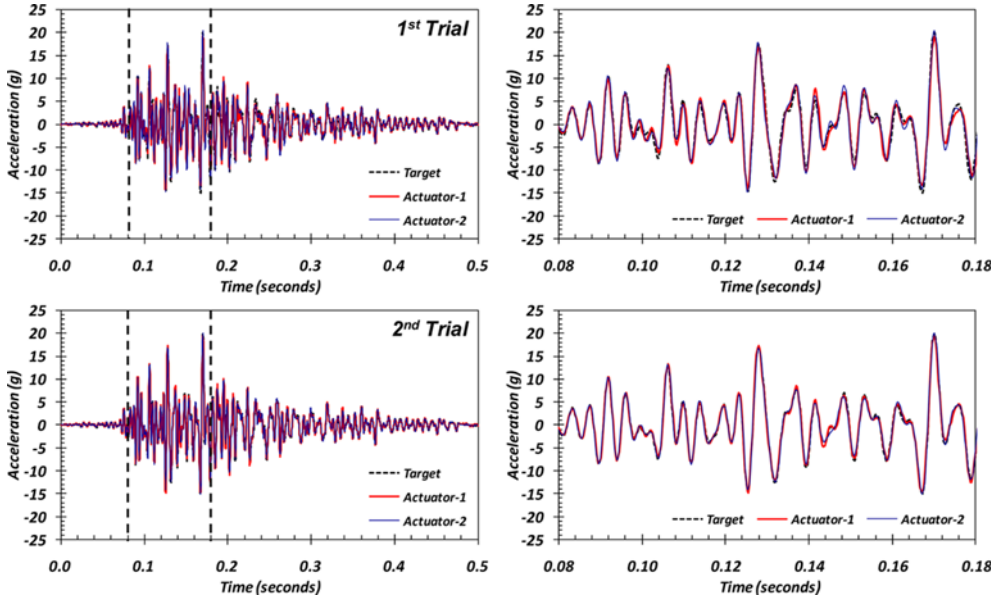

Fig. 8. Correction Process for Real Earthquake Motion

entire time. It is seen that the simulation and correction for real earthquake motion are easier than sine burst excitation due to its reduced consumption of power compared to sine burst.

3.3 Test Results with Sine Burst Excitations

A series of 1-second sinusoidal input signals were applied with various amplitudes and frequencies at a centrifugal acceleration of 60 gc. Hereafter, all test results are shown using acceleration motions compensated by the signal correction process described before. Fig. 9(a) shows a typical comparison of the target motion (Target-X) for a sinusoidal motion with 20gh amplitude and 160 Hz frequency and the measured motions at the both actuators (AX-1, AX-2) and the user slip table (Table-X). Measurements of only 0.08 s are shown for clear visualization. As shown in this figure, the measured responses nearly coincide with the target motion. In order to cover all test results obtained in this study, the error values on the RMS acceleration of Table-X relative to Target-X are noted in the performance envelop curve of this earthquake simulator, as shown in Fig. 9(b). The performance envelope plotted in Fig. 9(b) means theoretically achievable maximum performance with 1-second sinusoidal motion for a full payload of 700 kg in the absence of structural and hydraulic resonances. In this figure, the maximum shaking acceleration of the user slip table is plotted as a function of shaking frequency. At a low frequency range of less than 40 Hz, the 6.5 mm stroke of the actuator limits the shaking performance (stroke-limited), and at high frequency range greater than 200 Hz, it is constrained by the flow capacity of the hydraulic supply. This performance envelope is extremely useful for determining the sizes of the various parts of a hydraulic system during the design phase. In Fig. 9(b), the error values on *RMS* acceleration of table motions are within the limits of 5% for almost all test conditions. This is satisfied with a performance acceptance criterion adopted for the earthquake simulator at LCPC (Chazelas *et al*., 2008): error on the *RMS* acceleration of Table-X is less than 10% of that of Target-X. It can be mentioned that the user-desired target motions are reproduced at the actuators and the slip table with satisfactory fidelity.

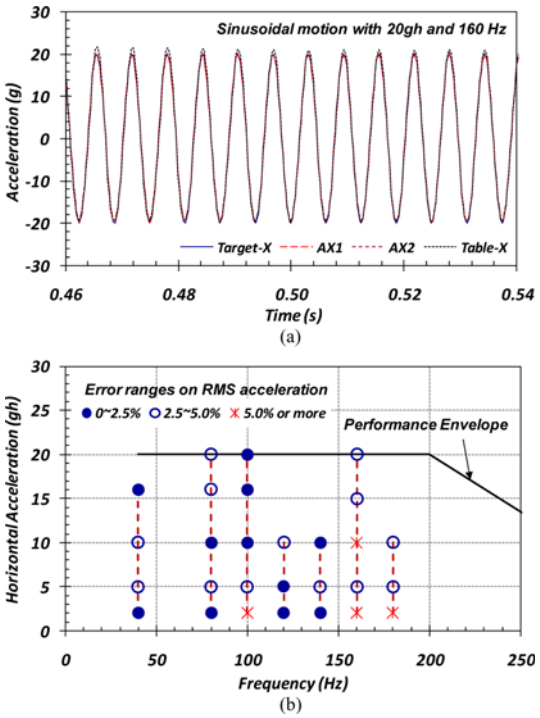

Fig. 9. Simulation Capacity of Target Sine Burst Excitation: (a) Typical Signals of Target-X, AX1, AX2, and Table-X, (b) RMS Error Ranges on Table-X Relative to Target-X

In addition, the table acceleration responses in the shaking direction (X-axis), which is indicated to Table-X in Fig. 5(b),

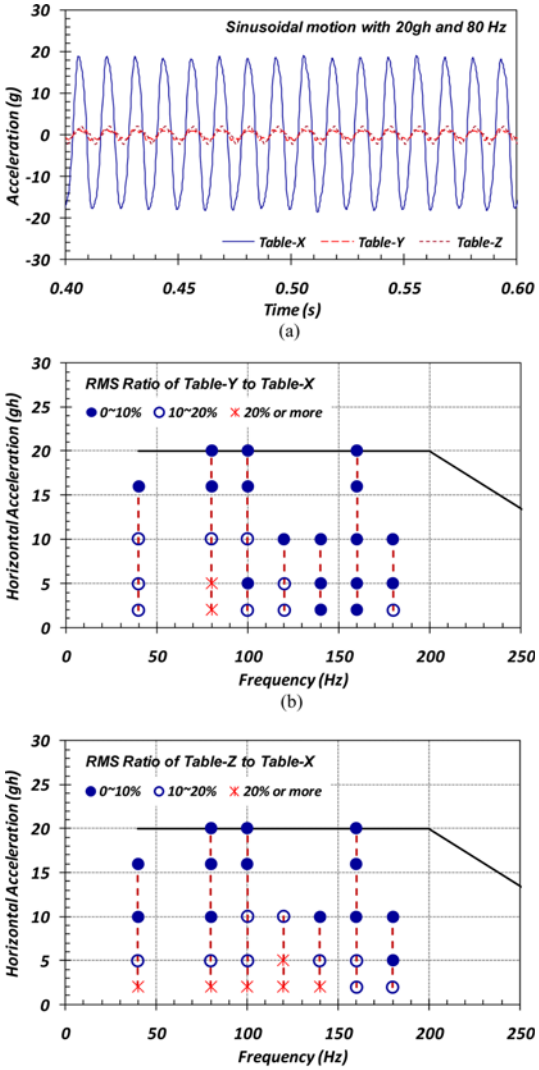

Fig. 10. Capacity Verification for Pure X-axis One-dimensional Table Excitation: (a) Typical Signals of Table-X, Table-Y, and Table-Z, (b) RMS Ratio Ranges of Table-Y (yawing) Relative to Table-X, (c) RMS Ratio Ranges of Table-Z (rocking) Relative to Table-X

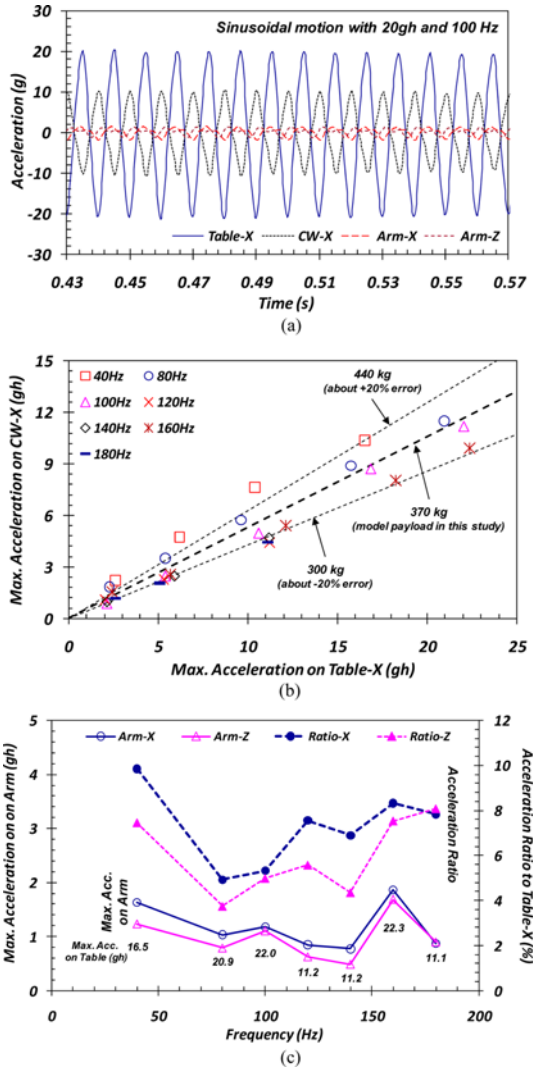

Fig. 11. Capacity Verification for Dynamic Self-balance and Vibration Insulation: (a) Typical Signals of Table-X, CW-X Arm-X, Arm-Z, (b) Maximum Accelerations of CW-X with the Corresponding Maximum Table-X, (c) Maximum Acceleration on Centrifuge Arm and Its Ratio to Maximum Table-X

were compared in the time and frequency domains with the coupled acceleration responses in the Y- and Z-axes (Table-Y and Table-Z). In order to obtain a precise response, it is essential that the non-shaking axis motions should be quite small and negligible during the one-dimensional excitation of the earthquake simulator. Fig. 10(a) shows a typical three-directional table responses recorded at the end of the slip table for an input motion with 20gh amplitude and 80 Hz frequency. The spurious responses, that is, Table-Y (yawing) and Table-Z (rocking) accelerations, have significantly reduced amplitudes as compared with the Table-X acceleration. The RMS ratio of the spurious responses to Table-X is calculated to 6.8% and 9.1% for Table-Y and Table-Z, respectively. The *RMS* ratio values were determined for all test cases performed in this study, and noted in the performance envelop curve, as shown in Figs. 10(b) and 10(c). The *RMS* ratio values of both spurious responses are within the 20% for most test conditions except for some of the low shaking accelerations, especially in Table-Z. This is not entirely satisfied with the second acceptance criterion proposed by Chazelas *et al.* (2008): the *RMS* acceleration of spurious motions (Table-Y and Table-Z) is less than 10% that of shaking motion (Table-X). However, it is expected to improve by performing a few more signal corrections. These results verify that the earthquake simulator can produce the pure one-dimensional base excitation.

The main features of this earthquake simulator are the dynamic self-balancing and the insulation of undesired vibrations between the user slip table and centrifuge swinging basket. These are achieved by employing the counter-weight platform and two hydraulic bearings as shown in Fig. 2. Fig. 11(a) shows the typical motions of the user slip table (Table-X), counter-weight

(CW-X), and centrifuge arm (Arm-X, Arm-Z) for an input motion with 20 gh amplitude and 100 Hz frequency. The measurements of only 0.14 s are shown for clear visualization. The CW-X motion has reduced amplitude with an exactly opposite phase as compared with the Table-X motion. The amplitudes of the maximum acceleration of Table-X and CW-X are around 22.1 gh and 11.8 gh, respectively. The ratio of acceleration amplitude is calculated to 1.87, and this value is similar with the inverse of the mass ratio between the model payload (370 kg) and the maximum testable model payload (700 kg). The mass difference between the counter-weights and user slip table is expected to be 700 kg. Consequently, the counteracting forces applied to the model payload and the counter-weight platform (F_{model} and F_{CW} in Fig. 2) are almost equal, and the residual torques applied to the centrifuge platform are expected to be negligible with the same levels of center of mass. It can be said that the dynamic self-balancing technique functions properly due to the model payload and the counter-weights. As a result, the maximum accelerations of the centrifuge arm (Arm-X, Arm-Z) are recorded to be around only 1gh, as shown in Fig. 11(a) in spite of the maximum shaking acceleration level (20 gh) of this earthquake simulator. The responses on the arm of centrifuge can be considered as negligible due to the dynamic self-balancing technique.

In order to investigate all of the test conditions, the maximum amplitudes of CW-X acceleration are plotted with the corresponding maximum amplitudes of Table-X in Fig. 11(b). In addition, the acceleration ratios corresponding to 370 kg (actual model payload used in this study), 300 kg (about -20% error), and 440 kg (about +20% error) are also plotted for comparison. The test results for 80 Hz and 100 Hz are consistent with the acceleration ratio of 370 kg, except that the low Table-X acceleration is less than 5 gh. However, there is a little difference in the other test results. The amplitudes of CW-X acceleration decrease with the increase of the frequency. Consequently, the unbalance may generate the undesired residual torques and then affect on the motions of centrifuge arm. For all of the tested frequencies, the maximum accelerations of Arm-X and Arm-Z at the tested maximum Table-X acceleration and its ratio to the Table-X are plotted in Fig. 11(c). Although the accelerations on the centrifuge arm were recorded as relatively large in the frequencies concerned with the unbalance, the acceleration and the ratio values are within the limits of 2 gh and 10%, respectively. These levels of acceleration and generated displacement are so weak that the risk of damage caused to the centrifuge structure may be negligible. This indicates that the dynamic self-balancing technique embarking the counter-weight platform sufficiently contributes to the safety of centrifuge structure.

3.4 Test Results with Real Earthquake Excitations

Prior to the sine burst excitations described in Section 3.3, the calibrated Northridge Earthquake excitations were performed not only to inspect the ability to perform multi-frequency inputs but also to investigate the boundary effects of the ESB model container. In the advance calibration process, the duration of the original earthquake motion was scaled to 0.5 s for the scaling of N=60, and the frequency contents were filtered by the limited frequency bandwidth between 40 Hz and 300 Hz. The maximum amplitudes were increased in stages from 2 gh to 20 gh.

For inspecting the capacity for real earthquake excitation, the responses for 20 gh amplitude excitation are shown as in Fig. 12 in a similar way to the interpretation of the above-mentioned sine burst excitation. The motions of Table-X and Target-X almost perfectly match through the whole excitation time including the part shown in Fig. 12(a). The spurious accelerations, Table-Y and Table-Z, have significantly reduced amplitudes as compared with the Table-X motion in both the time and frequency domains. It can be noticed that the dynamic self-balancing and vibration insulation are also properly functioned for this multi-frequency input motion. The responses of CW-X are maintained with the opposite phase to the Table-X as shown in Fig. 12(c)

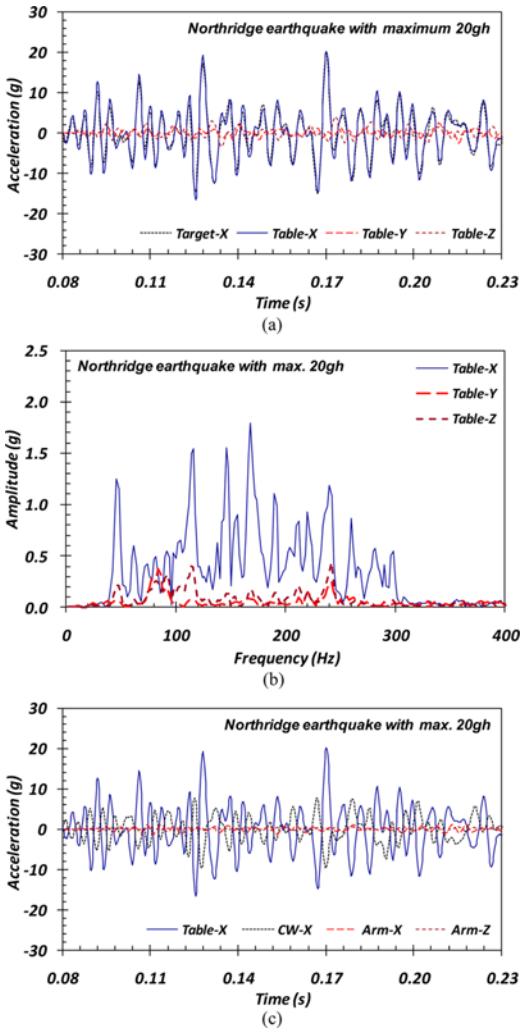

Fig. 12. Capacity Verification for Multi-frequency Earthquake Motion (Northridge Earthquake): (a) Typical Comparison of 3-directional Table Motions and Target-X of Maximum 20 gh Amplitude, (b) Table-X, Table-Y, and Table-Z in Frequency Domain, (c) Typical Signals of Table-X, CW-X, Arm-X, and Arm-Z

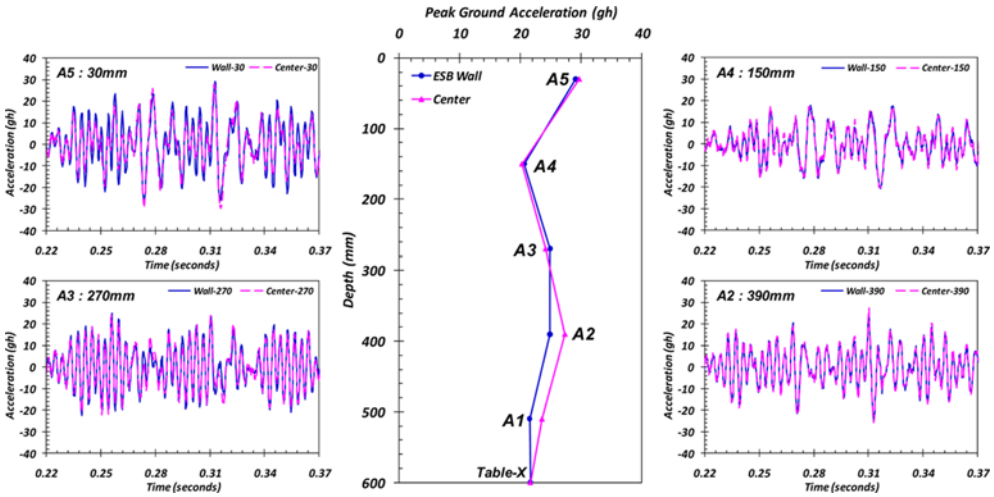

Fig. 13. Comparisons of Acceleration Time Histories and PGA with Depth between the End Wall of ESB Model Container and the Inside Soil Layer

and have reduced amplitudes due to the mass ratio between the model payload and the counter-weight platform. The maximum acceleration on Arm-X and Arm-Z are recorded to be less than only 1.5 gh, and this level of acceleration is expected to be negligible to the centrifuge structure.

The boundary effects of the ESB model container were investigated by comparing the responses on the Center and Wall arrays shown in Fig. 5(b). Fig. 13 shows typical acceleration time-histories and the corresponding PGA (peak ground acceleration) for the input motion of 20 gh amplitude. As shown in this figure, there is good agreement between the responses on the two accelerometer arrays. In time history, the two responses are almost identical in the acceleration amplitudes and time phases through the shown time range, except at some peaks in A5. It is expected that the amplitude differences at some peaks is caused by the soil settlements during previous shakings. From the test results, it can be said that the end walls of the ESB model container and the inside adjacent soil layers move together during shaking, and the ESB model container functions appropriately by minimizing the boundary effects. The details about verifying the performance of the ESB model container were demonstrated in Lee *et al*. (2013), where a series of dynamic centrifuge tests were performed at various soil conditions inside the ESB model container and the test results were compared with one-dimensional site response analyses to ensure the reliability of the test results.

4. Conclusions

A self-balanced electro-hydraulic earthquake simulator has been operated on the centrifuge in KAIST, which has an effective radius of 5 m and a maximum capacity of 240 g-ton. The earthquake simulator employed dynamic self-balancing technique in order to eliminate a large portion of the undesired reaction forces and vibrations transmitted to the centrifuge main body. The dynamic self-balancing was achieved by embarking counter-weight platform and two back-to-back hydraulic bearings. The details of the mechanical arrangement as well as the dynamic self-balancing technique were described in this paper.

A series of proof tests were conducted to examine the dynamic performance of the earthquake simulator and its excitation capacity for the mono-frequency sinusoidal and multi-frequency recorded earthquake inputs. In consequence of the test results, it was confirmed that the earthquake simulator can reproduce the user-desired target motions with satisfactory fidelity, and the dynamic self-balancing contributes to the safety of the centrifuge structure. The RMS error values on the slip table motions to the target motions are within the limits of 5% for almost test conditions. The non-shaking axis motions of the slip table, that is, Table-Y (yawing) and Table-Z (rocking) accelerations, have significantly reduced amplitudes as compared with on-axis Table-X acceleration. The dynamic self-balancing functions properly due to the counter-weight platform which moves to the opposite direction from the slip table. The counteracting forces applied to the model payload and counter-weight platform are almost identical, and the residual torques applied to the centrifuge platform are expected to be negligible. Consequently, the negligible levels of acceleration were recorded on the arm of the centrifuge, and the risk of damage caused to the centrifuge may be little.

Based on the good performance, the earthquake simulator will enable the worth studies on evaluating the seismic performance of geotechnical structures or soil-structure systems subjected to earthquake loading.

Acknowledgments

The authors gratefully acknowledge the KREONET service provided by Korea Institute of Science and Technology Information. This research was supported by Construction Technology Innovation

Program (11 Technology Innovation D02) from Construction Technology Innovation Program funded by Ministry of Land, Transport and Maritime Affairs of Korean government and the research program (grant number:2009-0080575) through the National Research Foundation of Korea (NRF) funded by the Ministry of Education, Science and Technology.

References

Chazelas, J. L., Escoffier, S., Garnier, J., Thorel, L., and Rault, G. (2008). "Original technologies for proven performances for the new LCPC earthquake simulator." *Bulletin of Earthquake Engineering*, Vol. 6, No. 4, pp. 723-728.

Elgamal, A., Yang, Z., Lai, T., Kutter, B. L., and Wilson, D. W. (2005). "Dynamic response of saturated dense sand in laminated centrifuge container." *Journal of Geotechnical and Geoenvironmental Engineering,* ASCE, Vol. 131, No. 5, pp. 598-609.

Ghosh, B. and Madabhushi, S. P. G. (2007). "Centrifuge modelling of seismic soil structure interaction effects." *Nuclear Engineering and Design*., Vol. 237, No. 8, pp. 887-896.

Hutin, C., Perdriat, J., and Rames, D. (2002). "Dynamically balanced broad frequency earthquake simulation." *Proceedings of the International Conference on Physical Modelling in Geotechnics: ICPMG'02*, July 10-12, Newfoundland, Canada, pp. 175-178.

Kim, D. S., Kim, N. R., Choo, Y. W., and Cho, G. C. (2013). "A newly developed state-of-the-art geotechnical centrifuge in Korea." *KSCE Journal of Civil Engineering*, Vol. 17, No. 1, pp. 77-84.

Kutter, B. L., Idriss, I. M., Khonke, T., Lakeland, J., Li, X. S., Sluis, W., Zeng, X., Tauscher, R. C., Goto, Y., and Kubodera, L. (1994). "Design of a large earthquake simulator at UC Davis." *Centrifuge 94-Proceedings of the International Conference Centrifuge 94*, Singapore, pp. 169-175.

Kutter, B. L. and Wilson, D. W. (2006). "Physical modelling of dynamic behavior of soil-foundation-superstructure systems." *International Journal of Physical Modelling in Geotechmics,* Vol. 6, No. 1, pp. 1-12.

Lee, S. H., Choo, Y. W., and Kim, D. S. (2013). "Performance of an Equivalent Shear Beam (ESB) model container for dynamic geotechnical centrifuge tests." *Soil Dynamics and Earthquake Engineering*, Vol. 44, pp. 102-114.

Perdriat, J., Phillips, R., Nicolas Font, J., and Hutin, C. (2002). "Dynamically balanced broad frequency earthquake simulation system." *Proceedings of the International Conference on Physical Modelling in Geotechnics: ICPMG'02*, July 10-12, Newfoundland, Canada, pp. 169-173.

Schofield, A. N. and Zeng, X. (1992). *Design and performance of an equivalent shear beam (ESB) container for earthquake centrifuge modelling*, Technical Report TR245, Cambridge: Department of Engineering, University of Cambridge.

Shen, C. K., Li, X. S., Ng, C. W. W., Van Laak, P. A., Kutter, B. L., Cappel, K., and Tauscher, R. C. (1998). "Development of a geotechnical centrifuge in Hong Kong." *Centrifuge 98-Proceedings of the International Conference Centrifuge 98*, Tokyo, Japan, pp. 13-18.

Takemura, J., Takahashi, A., and Aoki, Y. (2002). "Development of horizontal-vertical 2D shaker in a centrifuge." *Proceedings of the International Conference on Physical Modelling in Geotechnics: ICPMG'02*, July 10-12, Newfoundland, Canada, pp. 163-168.

Taylor, R. N. (1995). *Geotechnical centrifuge technology*, 1st Edition, Blackie Academic and Professional.

Ueng, T. S., Wu, C. W., Cheng, H. W., and Chen, C. H. (2010). "Settlements of saturated clean sand deposits in shaking table tests." *Soil Dynamics and Earthquake Engineering*, Vol. 30, Nos. 1-2, pp. 50-60.

Wood, D. M., Crewe, A., and Taylor, C. (2002). "Shaking table testing of geotechnical models." *International Journal of Physical Modelling in Geotechmics*, Vol. 2, No. 1, pp. 1-13.

Yu, Y., Deng, L., Sun, X., and Lu, H. (2008). "Centrifuge modeling of a dry sandy slope response to earthquake loading." *Bulletin of Earthquake Engineering*, Vol. 6, No. 3, pp. 447-461.

Zehgal, M., Dobry, R., Abdoun, T., Zimmie, T. F., and Elgamal, A. (2002). "NEES earthquake simulation and networking capabilities at RPI centrifuge." *Proceedings of the 7th U.S. National Conference on Earthquake Engineering (7NCEE)*, July 21-25, Boston, USA (in CD-ROM).